

A scan of the Galactic plane in the TeV-band with the HEGRA stereoscopic IACT system

G. Pühlhofer¹, K. Bernlöhr^{1,2}, A. Daum¹, for the HEGRA Collaboration

¹Max-Planck-Institut für Kernphysik, Saupfercheckweg 1, D-69117 Heidelberg

²Forschungszentrum Karlsruhe, D-76021 Karlsruhe

Abstract

Usually, Cherenkov telescopes are used to observe sources which are well established in other wavelength bands. The limited sensitivity of present instruments leads to the fact that most of the sky has never been examined in the TeV band. The HEGRA stereoscopic IACT system is for the first time able to perform scans of extended sky regions with a sensitivity for point sources well below the Crab flux. As a first target for such a scan, part of the Galactic disk was examined. The campaign took ≈ 130 hrs of observation time in 1997/98. The observations extended from the Galactic center to the local arm of our Galaxy, where the sun is located ($0^\circ < l < 83.5^\circ$, $\Delta b = 2^\circ$). This region was chosen because of the high concentration of several types of source populations. A first data analysis reveals no hints for strong TeV point sources.

1 Introduction

A full sky survey in the TeV wavelength band is still out of reach for the present generation of Cherenkov telescopes. However, with the HEGRA stereoscopic system of Imaging Atmospheric Cherenkov Telescopes (IACT), scans of extended sky regions with a sensitivity of well below the Crab flux have become possible within reasonable time. The scan capabilities are due to an essentially background-free detection of TeV gamma ray point sources of down to 1/4 Crab within one hour, and the effective field of view (FOV) of more than 2° diameter with nearly homogeneous acceptance for TeV gamma rays.

As a first target for such a scan, part of the Galactic disk was studied. Observations were mainly centered along the Galactic plane, running from the Galactic center ($l > -1.5^\circ$) to the Cygnus region ($l < 83.5^\circ$). The observed regions can be characterized as follows:

1. The region from the Galactic center to the edge of the inner part of the Galaxy ($l < 54^\circ$). The search aims for absolutely bright but distant sources (distance to the Galactic center is 8.5 kpc).
2. The Cygnus region ($73.5^\circ < l < 83.5^\circ$). This is a view along the local spiral arm of our Galaxy. A length-scale of 1-2 kpc is hereby scanned. In principle also our local surroundings are seen here, but of course only a small part of it; as the local area extends a major part of the hemisphere, a full scan is currently out of reach.
3. The region inbetween these two ($54^\circ < l < 73.5^\circ$). This is a view between the local arm and the inner part of the Galaxy, with low HII and EGRET γ -ray emissions. Here the scan basically follows a path of relatively high density of source candidates mainly supernova remnants.

2 Observations

Regions 1 and 2 were observed during summer 1997, the scan was continued with region 3 during summer 1998. All observations were taken with the 4-telescope setup of the HEGRA IACT system (for a short detector description see Aharonian et al., 1999b, OG.2.1.16, the detector performance is described e.g. in Aharonian et al., 1999a). During the 1998 data taking the system had a slightly increased energy threshold (+15%) plus an increased detector dead time, which resulted in a decreased system trigger rate.

The scan was performed such that each point within the searched area was observed for at least 2 hours. The scan of region 1 (inner part of the Galaxy) follows basically the Galactic plane, producing a band of $\Delta b = 2^\circ$. Triggered by a fast analysis, reobservations of some spots within this search window were performed already during this observation campaign. Region 2 covers most parts of the Cygnus region, with Δb up to 5° . Region 3 again covers a band of $\Delta b = 2^\circ$, leaving the Galactic plane when approaching the Cygnus region. The

observational positions are shown in figure 1. Each circle represents the accepted FOV, during each data run (30 min) the telescopes were tracking the respective position of the Galactic plane. The total observation time under accepted observation conditions was 105 hrs.

For Galactic longitudes smaller than 30° , the Galactic disk culminates at zenith angles larger than 30° at La Palma site. The Galactic center can only be observed at 60° zenith angle. All observations were made close to culmination in order to ensure minimum zenith angle, and thereby optimum sensitivity and energy threshold (for the zenith angle dependence of the system energy threshold see Konopelko et al., 1999, Konopelko, & Pühlhofer, 1999).

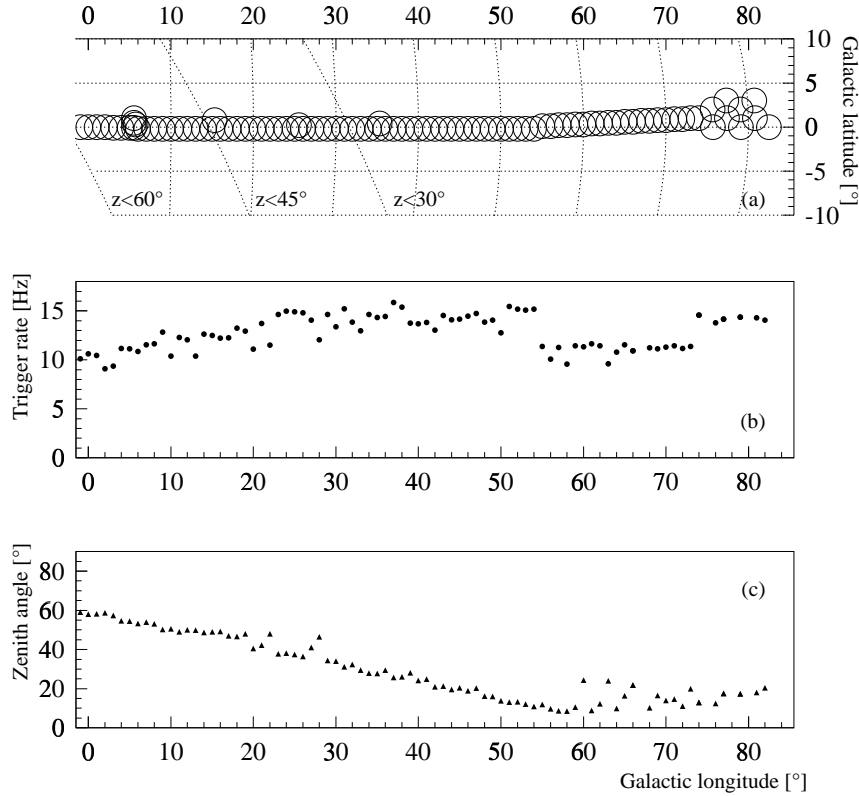


Figure 1: (a) Observed regions in Galactic coordinates. The circles indicate the field of view of the telescope system. The diagonal lines mark culmination zenith angles (from left to right) 60° , 45° and 30° . (b) Mean trigger rates. (c) Zenith angles of the observations.

3 Analysis Methods and Results

The analysis presented here focuses on the search for point sources. An approach to a possible search for diffuse gamma-ray emission is given in Lampeitl et al. 1999, OG.2.4.12.

Each individual event, induced by a TeV gamma or Cosmic ray (CR), is stereoscopically reconstructed. The direction of primary gamma rays is determined with an accuracy of 0.09° per event, with a systematic pointing accuracy of better than 0.01° (Pühlhofer et al., 1997). The shower core, which is the projected impact point of the primary onto the ground, is reconstructed with an accuracy of 10-15 m. All events within a radius of $r = 1.2^\circ$ from the center of the FOV were accepted.

In order to eliminate the background produced by CR induced events, the shower image shapes as measured under different viewing angles with different telescopes, are compared to expectation values, taking into ac-

count the measured image amplitudes, the distance of the telescopes to the measured shower core, and zenith angle. Two different shape cuts were applied in this analysis:

A: A combined cut on the so called *mean scaled width* $\langle \tilde{w} \rangle$ (Aharonian et al. 1999a) and the analogous *mean scaled length* $\langle \tilde{l} \rangle$ (see also Konopelko, & Pühlhofer, 1999, OG 2.2.01). This cut ensures homogeneous gamma ray acceptance over the full zenith angle range.

B: A probability cut, that calculates the probability that the primary particle was a gamma or CR, by comparing the image shapes to gamma and to CR expectations (Daum et al., 1997, Pühlhofer et al., 1999, OG 2.2.01). Studies of systematic uncertainties of gamma ray efficiencies, especially at large zenith angle, are still in progress.

For both methods, the selected gamma ray candidates are filled in bins of $0.1^\circ \times 0.1^\circ$ in the Galactic coordinate system, which is the event resolution for single gamma ray events.

The optimum search window with a radius of 0.14° is approximated by summing up the bin contents over an area of $0.3^\circ \times 0.3^\circ$ into a new grid of $0.1^\circ \times 0.1^\circ$ spacing.

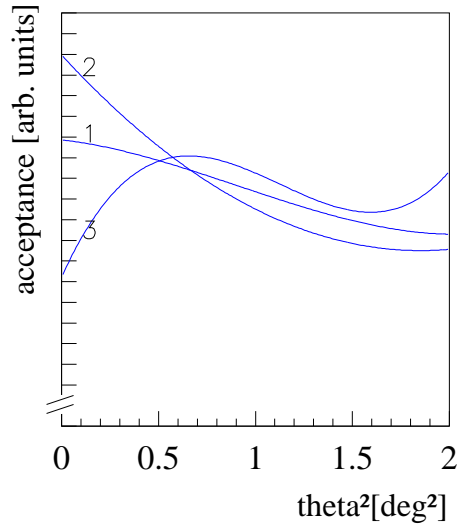


Figure 2: Field of view acceptance as used for background estimation: (1) trigger acceptance (no image selection), (2) after cuts A (see text), (3) after cuts B. Acceptance is given in arbitrary units. Note the offset at the y-axis.

The background distribution is computed by convoluting the background rate after cuts of each data run with the slightly inhomogeneous background acceptance (see figure 2). In order to minimize statistical errors on the background rates, and systematic effects due to possible extended TeV-emitting regions, the accepted FOV for background counting was enlarged to $r = 1.4^\circ$. The expected impact of diffuse emission is anyway low, see Lampeitl et al. 1999, OG.2.4.12.

Finally, for each point the chance probability of the count rate being due to background fluctuation (using Poisson statistics) is calculated. The resulting probability distributions in the $0.1^\circ \times 0.1^\circ$ binned samples for both shape cuts were found to be flat, i.e. in agreement with the background expectation. This provides a check of the analysis, and highly significant sources would already show up here. The $0.3^\circ \times 0.3^\circ$ rebinned distributions are not flat as expected, since the individual points are correlated. This does not basically affect the search for points with high excess significance: any 'hot spots' would just show up a few times in the probability distributions with high statistical significance.

The scan yielded no source candidate, since no point with excess significance below 1×10^{-4} was found. Given the total number of search points of ≈ 21000 , this is in agreement with statistical background fluctua-

tions. Hence the scan yields an upper limit on the examined regions of 1/4 Crab at Galactic longitudes above 30° . Further studies on detector and cut efficiencies, especially at large zenith angles, are under way.

References

- Aharonian, F., et al. 1999a, *A&A* 342, 69
Aharonian, F., et al. 1999b, Proc. 26th ICRC (Salt Lake City), OG.2.1.16
Daum, A., et al. 1997, *Astrop. Phys.* 8, 1.
Konopelko, A., et al. 1999, submitted to *J. Phys. G*.
Konopelko, A., & Pühlhofer, G. 1999, Proc. 26th ICRC (Salt Lake City), OG 2.2.01
Lampeitl, H., & Konopelko, A. 1999, Proc. 26th ICRC (Salt Lake City), OG.2.4.12
Pühlhofer, G. et al. 1997, *Astrop. Phys.* 8, 101-108
Pühlhofer, G., Völk, H.J., & Wiedner, C.A. 1999, Proc. 26th ICRC (Salt Lake City), OG 2.2.01